



Tóth, B., Janacsek, K., Takács, Á., Kóbor, A., Zavecz, Z. and Nemeth, D. (2017)
Dynamics of EEG functional connectivity during statistical learning. *Neurobiology of Learning and Memory*, 144, pp. 216-229.

There may be differences between this version and the published version. You are advised to consult the publisher's version if you wish to cite from it.

<http://eprints.gla.ac.uk/146564/>

Deposited on: 13 September 2017

Enlighten – Research publications by members of the University of Glasgow
<http://eprints.gla.ac.uk>

Dynamics of EEG functional connectivity during statistical learning

Brigitta Tóth^{1,4,*}, Karolina Janacsek^{1,2,*}, Ádám Takács^{2,5*}, Andrea Kóbor^{3,*}, Zsófia Zavecz^{1,2},
Dezso Nemeth^{1,2*}

1. Institute of Cognitive Neuroscience and Psychology, Research Centre for Natural Sciences, Hungarian Academy of Sciences, *Magyar tudósok körútja 2., H-1117, Budapest, Hungary*
2. Institute of Psychology, Eötvös Loránd University, *Izabella u. 46., H-1064, Budapest, Hungary*
3. Brain Imaging Centre, Research Centre for Natural Sciences, Hungarian Academy of Sciences, *Magyar tudósok körútja 2., H-1117, Budapest, Hungary*
4. Center for Computational Neuroscience and Neural Technology, Boston University, *677 Beacon St, MA 02215, Boston, USA*
5. Institute of Neuroscience and Psychology, University of Glasgow, Hillhead street 58, G12 8QB, Glasgow, United Kingdom

*These authors contributed equally to this work.

Manuscript of the article that appeared in:

Neurobiology of Learning and Memory 2017; 144C: 216-229

DOI: 10.1016/j.nlm.2017.07.015

Author Note

Correspondence concerning this article should be addressed to Dezso Nemeth, Institute of Psychology, Eötvös Loránd University, Izabella u. 46., H-1064, Budapest, Hungary. Telephone: +36703189107. E-mail address: nemeth@nemethlab.com, toth.brigitta@ttk.mta.hu

Abstract

Statistical learning is a fundamental mechanism of the brain, which extracts and represents regularities of our environment. Statistical learning is crucial in predictive processing, and in the acquisition of perceptual, motor, cognitive, and social skills. Although previous studies have revealed competitive neurocognitive processes underlying statistical learning, the neural communication of the related brain regions (functional connectivity, FC) has not yet been investigated. The present study aimed to fill this gap by investigating FC networks that promote statistical learning in humans. Young adults ($N = 28$) performed a statistical learning task while 128-channels EEG was acquired. The task involved probabilistic sequences, which enabled to measure incidental/implicit learning of conditional probabilities. Phase synchronization in seven frequency bands was used to quantify FC between cortical regions during the first, second, and third periods of the learning task, respectively. Here we show that statistical learning is negatively correlated with FC of the anterior brain regions in slow (theta) and fast (beta) oscillations. These negative correlations increased as the learning progressed. Our findings provide evidence that dynamic antagonist brain networks serve a hallmark of statistical learning.

Keywords: EEG, functional connectivity, implicit learning, phase synchronization, predictive processing, statistical learning

Introduction

Statistical learning is a fundamental mechanism of the brain, which extracts and represents regularities of our environment enabling predictive processing during perception and acquisition of perceptual, motor, cognitive, and social skills (Armstrong, Frost & Christiansen, 2017; Aslin, 2017; Cleeremans & McClelland, 1991; Reber, 1967). Learning statistical probabilities of environmental stimuli induces structural and functional plasticity in the nervous system (Fiser et al., 2010). The related neuronal activity changes involve temporary and/or permanent influences on the functional networks required for task performance (Bassett et al., 2011). Although previous electrophysiological and neuroimaging studies (Bassett et al., 2011; Fell & Axmacher, 2011; Poldrack et al., 2001; Schapiro, Gregory, Landau, McCloskey, & Turk-Browne, 2014; Stillman et al., 2013) have revealed a distributed network of brain regions underlying learning, the related neural communication (termed as “functional connectivity”) of these cortices has not yet been investigated. The aim of the present EEG study was to explore inter-regional functional connectivity in humans during statistical learning and test its relationship with individual’s learning capacity.

Previous neuroimaging research has shown that neurocognitive networks underlying learning can interact in a cooperative or a competitive way (Poldrack et al., 2001; Schwabe & Wolf, 2013). A growing number of behavioral and brain imaging research demonstrated that weaker frontal lobe-dependent executive and control functions were associated with better learning performance in tasks consisting probabilistic properties (Filoteo et al., 2010; Nemeth, Janacsek, Polner, & Kovacs, 2013; Virag et al., 2015). It could be interpreted by assuming a competitive-antagonist relationship between controlled, expectation-driven and automatic, stimulus-driven learning processes, where greater involvement of the former processes may interfere with the extraction of the statistical properties of the environment (Janacsek, Fiser, & Nemeth, 2012; Daw,

Niv, & Dayan, 2005; Daw, Gershman, Seymour, Dayan, & Dolan, 2011). For instance, Nemeth and colleagues (2013) observed better statistical learning using hypnotic instructions as an experimental manipulation that reduced control functions. It was assumed that control functions declined via weakened functional connections of the frontal cortices. However, in spite of the interactions found both on the behavioral and on the neural level in the above- mentioned studies, FC during statistical learning has not yet been directly investigated.

Evidence from recordings of electrical activity in humans and animals suggest that cortical computations of memory encoding can be described by rhythmic shifting of neuronal excitability over a wide range of spatial and temporal scales (termed as neural oscillations, for reviews, see Varela 2001; Caplan, & Glaholt, 2007; Klimesch, Freunberger, Sauseng, & Gruber, 2008; Mitchell, McNaughton, Flanagan, & Kirk, 2008; Kikuchi et al., 2017). Theta (4–7 Hz) and coupled gamma (< 30 Hz) activity in the rodent hippocampal formation was suggested to underlie spatial representation, memory, and consolidation (for review, see Buzsáki 2005). In humans, theta oscillations (4–7 Hz) were consistently observed particularly within the fronto-midline regions during the retention of information in working memory and also during reorientation or allocation of attention to the sensory stimuli (for example, Onton, Delorme, & Makeig, 2005; Gevins et al., 1997; Hsieh et al., 2011; Jensen & Tesche, 2002; Raghavachari et al., 2001; Scheeringa et al., 2009; Tóth et al. 2014). Converging evidence suggests that theta oscillations are related to encoding and retrieval processes of the long-term declarative memory (for review see Hsieh & Ranganath, 2014; Meyer et al., 2015). Neural responses during procedural learning in tasks that require processes of sequences or/and statistical regularities, however, have received substantially less attention. For instance, motor sequence learning has been associated with changes of alpha and beta band oscillatory activity (Bassett et al., 2011; Fell & Axmacher, 2011; Stillman et al., 2013). In another sequence learning study (Pollock et al., 2014), the authors found stepwise decline of alpha band

event related desynchronization with faster reaction times. The reduction of reaction times was significantly correlated with the amount of beta-band suppression.

It has recently been realized that rather than the event related activity of single brain regions, the induced and sustained inter-regional functional connectivity is an ideal candidate to measure cooperative or competitive parallel processes that underlie statistical learning (Fell & Axmacher, 2011). By supporting sustained coordinated timing of neuronal firing between distant cortical areas, oscillatory synchronization integrates anatomically distributed processing and facilitates neuronal communication, thereby supports synaptic plasticity (Buzsaki & Draguhn, 2004). To date, there is only a single neuroimaging and no electrophysiological study that investigates the functional connectivity correlates of statistical learning. Consequently, the nature of the underlying functional networks supporting an individual's capacity for statistical information encoding remains poorly understood. The brain imaging study of Bassett et al (2011) showed that the organization of FCs during learning provides critical insight into the underlying neural architecture: they have identified a modular structure in the human brain function during learning over a scales from minutes to days; this FC organization was modulated by early learning, varied over individuals, and was a significant predictor of learning in subsequent experimental sessions (Bassett et al. 2011).

The main objective of the present study was to test the relationship between inter-regional FC (measured as oscillatory phase synchronization in EEG) and statistical learning. In order to obtain high-density data (reaction time and accuracy) of the statistical learning performance, we used a perceptual-motor probabilistic sequence learning task (Janacsek et al., 2015). Based on the assumption of inverse-antagonist relation (Filoteo et al., 2010; Nemeth et al., 2013; Virag et al., 2015), it was hypothesized that the weaker FC of the fronto-central cortices and between frontal and posterior cortices would promote the better acquisition of probabilistic information. Since our

study is the first investigating EEG FC related to statistical learning, the second objective was to explore dynamical correspondence between learning performance and FC properties.

Material and Methods

Participants

Thirty-one healthy young adults (18-30 years; $M = 25.04$, $SD = 6.77$ years; mean education: $M = 16.36$, $SD = 2.39$ years; male/female ratio: 5/23) participated in the study. All of them were right-handed and had normal or corrected-to-normal vision. They did not report active neurological or psychiatric conditions, were not taking any psychoactive medications, and performed in the normal range on standard neuropsychological tests (Counting Span task: $M = 3.57$, $SD = 0.84$; Letter Fluency task: $M = 17.12$, $SD = 4.55$; Semantic Fluency task: $M = 26.92$, $SD = 7.22$). All participants signed an informed consent and received course credit for participation. The study was conducted in full accordance with the World Medical Association Helsinki Declaration and all applicable national laws; the study was approved by the relevant ethics committee. Three participants were excluded from the analysis based on the minimum epoch number criterion (50 per participant, separately for each learning period, see section EEG data in Data analysis); therefore, the final sample consisted of 28 participants.

Alternating Serial Reaction Time task (ASRT)

Statistical learning was measured by the Alternating Serial Reaction Time (ASRT) task (Nemeth et al., 2010; Howard & Howard, 1997). In this task, four empty circles (black line drawings, 300 pixels each) were presented continuously on a white background in a horizontal arrangement in the middle of the screen. A target stimulus (a picture of the head of a dog, 300 pixels) presented

sequentially in one of the four empty circles (see in Figure 1). The stimulus was presented at 5° of angle of vision (monitor resolution was 1280*1024 pixels with 60 Hz refreshment rate; the viewing distance from the monitor was 80 cm). Participants were instructed to press a button corresponding to the target position as quickly and as accurately as they could. A keyboard with four heightened keys (Z, C, B, and M on a QWERTY keyboard) was used as a response device, each of the four keys corresponding to the circles in a horizontal arrangement. Participants were asked to respond with their middle- and index-fingers of both hands.

Importantly, the serial order of the four possible positions (coded as 1, 2, 3, and 4) in which target stimuli could appear was determined by an eight-element probabilistic sequence (see in Figure 1). In this sequence, every second element's position was fixed and repeated sequentially in the same order as the task progressed, while the other elements' positions were randomly chosen out of the four possible locations (e.g., 2r4r3r1r; r denotes the random position). Due to this probabilistic sequential structure of stimuli appearance, some combinations of three consecutive trials (so-called "triplets") occur more frequently than others (the former is referred to as high-probability triplets and the latter as low-probability triplets). For example, in the above illustration, 2_4, 4_3, 3_1, and 1_2 (where "_" indicates any possible middle element of the triplet) would occur often because the third element (bold numbers) could be derived from the sequence or occasionally could be a random element as well. In contrast, 1_3 or 4_2 would occur less frequently because in this case, the third element could only be random (Figure 1). Note that the final event of high-probability triplets was, therefore, more predictable from the first event when compared to the low-probability triplets [also known as a non-adjacent second-order dependency (Remillard, 2008)]. Therefore, for each stimulus we determined whether it was the last element of a high- or low-probability triplet. There were 64 possible triplets (four stimuli combined for three consecutive events) in the task. Out of these triplets, 16 were high-probability triplets, each of them occurring

in approximately 4% of the trials, about five times more often than the low-probability triplets. Thus, approximately 62.5% of all trials were high-probability triplets and the remaining 37.5% of trials were low-probability ones.

Previous studies have shown that as people practice the ASRT task, responses become faster and more accurate to the high- than to low-probability triplets, revealing statistical learning (Howard & Howard, 1997; Howard et al., 2004; Song et al., 2007a). Note that since statistical learning is defined as the *difference* in responses to high- vs. low probability triplets, gaining knowledge of this statistical structure is independent of overall RT and accuracy improvements (often termed as general skill learning), which are related to improving visuomotor and motor-motor coordination during practice. Thus, by using the ASRT task, we were able to obtain a statistical learning measure independently of general skill improvements. Although we present the behavioral results for both general skill improvements and statistical learning, in the current study, we focus only on the relationship between statistical learning measures (*difference* in responses to high- vs. low probability triplets) and EEG FC during learning.

Procedure

The timing of the task was the following. First, at the beginning of a block, a screen with the four empty circles was shown for 200 ms which was followed by the presentation of a target stimulus. Participants were required to respond within 500 ms by pressing the button that corresponded to the target location. The target remained on the screen for 500 ms, irrespective of the participant's response time. Before the next trial, a 120 ms long inter-stimulus-interval was inserted where a screen with the four empty circles was shown. Stimuli were presented in blocks of 85 trials, where the first five trials were random, serving warm-up purposes, then an eight-element probabilistic sequence was repeated ten times. After each block, participants received feedback about their

overall reaction time and accuracy in the given block. The feedback lasted for 5000 ms and was followed by a 2000 ms long delay interval while the participant could have a short rest. The task consisted of 35 blocks. As one block took about 1-1.5 min, the entire session took approximately 35-45 min. There were six possible probabilistic sequences based on a permutation of the four possible positions, and sequences were counterbalanced across subjects (Nemeth et al., 2010, Song et al., 2007b).

To explore how much explicit knowledge participants acquired about the task, we administered a short questionnaire after the session (Nemeth et al., 2010; Song et al., 2007b). The questionnaire included increasingly specific questions such as “Have you noticed anything special regarding the task?”, “Have you noticed any regularity in the sequence of the stimuli?” None of the participants reported noticing the sequence structure of the stimulus stream. In addition, previous studies – using verbal reports, free generation (inclusion condition) and triplet sorting tasks – have shown that participants remain unaware of the stimulus structure if it is not explicitly cued (e.g., Song, Howard, & Howard, 2007a) and even after extended practice (e.g., ten days; D. V. Howard et al., 2004). Based on the previous ASRT studies, and the results of the verbal reports in the current study, we believe that participants did not gain explicit knowledge of the alternating sequence.

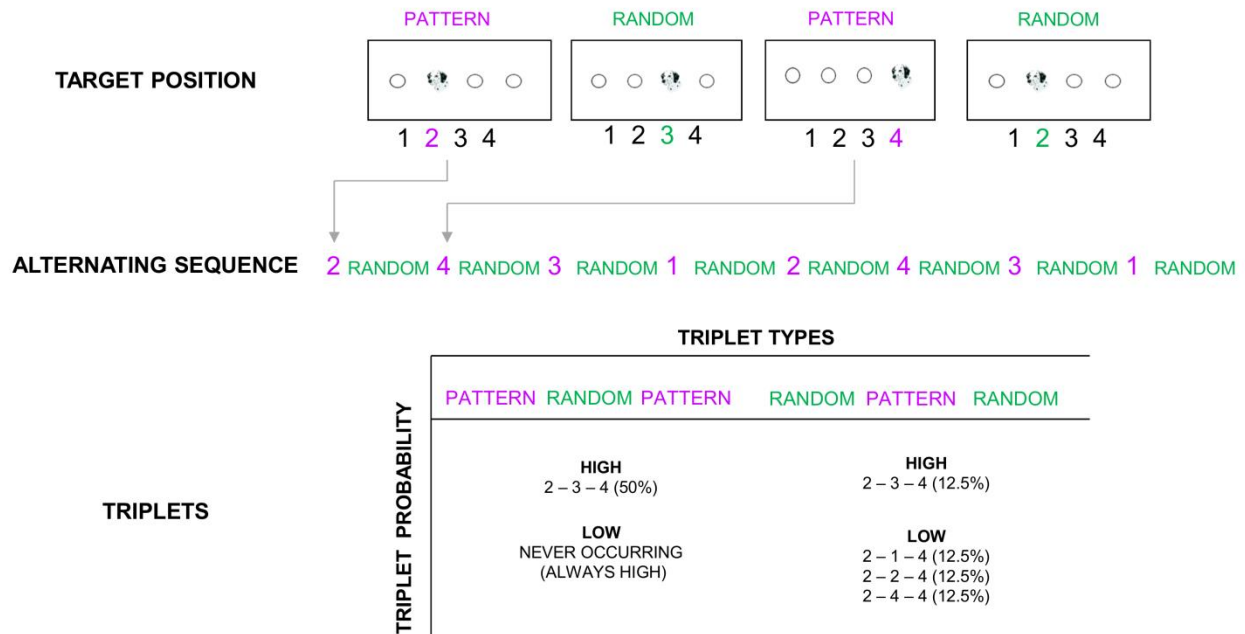


Figure 1. The statistical structure of the ASRT sequence. As a result of the alternation of pattern (magenta) and random (green) trials, there are more probable and less probable combinations of three consecutive stimuli. Based on the first two elements are of such a combination (referred to as triplets), there is always a probable continuation (*high-probability triplets*), and three less probable continuations (*low-probability triplets*). As pattern trials take up 50% of all trials, and they always appear in the same order, they always form high-probability triplets. Random trials by chance (1/4 of the remaining 50% of trials, thus 12.5%) can form the same high-probability triplets as the pattern trials, adding up to 62.5% of all trials being high-probability triplets. The remaining 37.5% of the trials are low-probability triplets.

EEG data collection

The study was conducted in an acoustically attenuated, dimly lit room. A 19-inch monitor was placed in front of the participants. EEG was recorded using the Electrical Geodesics system with 128-channel HydroCel Geodesic Sensor Net (GES 300; Electrical Geodesics, Inc.) and Net Station 4.5.1 software. Electrode impedance levels were kept below 50 kΩ, and 100 Hz online low pass filter was applied. Cz served as a reference and sampling rate of 1000 Hz was used for recordings.

Data analysis

Behavioral data

To increase statistical power, we analyzed periods (clusters of blocks) rather than single blocks. The first period consisted of 11 blocks (blocks 1-11), the second and the third periods consisted of 12 blocks in each (blocks 12-23 and blocks 24-35, respectively). Mean accuracy (ratio of correct responses) and median reaction time (RT for correct responses) were calculated for each participant and period, separately for high- and low-probability triplets. For each period, a learning score was also calculated as the difference between triplet types in RT (RT for low-probability triplets minus RT for high-probability triplets) and accuracy (accuracy for high-probability triplets minus accuracy for low-probability triplets). These learning scores were then averaged across the three periods resulting in two *overall learning score* indices (for RT and accuracy, respectively). Greater learning score in both measures indicates greater statistical learning.

To evaluate performance changes due to statistical learning, we conducted repeated measures analyses of variance (ANOVAs – see detailed description below) separately for accuracy and RT. Greenhouse-Geisser epsilon (ϵ) correction was used if necessary. Original *df* values and corrected *p* values (if applicable) are reported together with partial eta-squared (η_p^2) as the measure of effect size.

EEG data

All EEG data preprocessing was done with EEGLab toolbox (12_0_2_0b version, Delorme et. al., 2007) of Matlab software (Matlab 2013a). Data was offline band-pass filtered between the 0.5-45 Hz frequency range using Hamming windowed finite-impulse-response filter (roll of speed -53dB; maximum bandpass deviation 0.0022). The EEG recorded during the ASRT blocks was trisected into three periods consisting of approximately equal time intervals (first period consisting

of blocks 1-11, the second period consisting of blocks 12-23, and third period consisting of blocks 24-35, in accordance with the behavioral data). The feedback periods of the task and the resting periods between blocks was discarded from the analysis. Since the same number of motor responses were executed within each block (see section Procedure), the amount of movement related EEG activity (i.e., within the beta band) did not differ across the time periods.

EEG signal was visually screened for high amplitude non-eye-movement related artifacts due to body movements, sweating, and temporary electrode malfunction. Maximum six bad channels (less than 5 % of all EEG channels) per participants were interpolated. Those EEG segments in which the artifacts could not be removed with the ICA procedure (applied for removing blink artifacts, see below and Delorme et. al., 2007) were rejected from the analysis.

The EEG signal with ocular types of artifacts (horizontal and vertical eye-movement) was identified and removed by infomax algorithm of independent component analysis (option: binica). ADJUST automatic classification algorithm (EEGlab plugin, version 3, Mognon et al., 2010; Delorme et. al., 2007) was employed that can detect independent components of artifacts based on stereotyped spatial and temporal features. ICA components constituting blink artifacts were removed via visual inspection of their topographical distribution and frequency contents. Maximum six independent components per participants were removed. These artifacts can be removed from the data without affecting the activity of neural sources of the relevant frequency bands, i.e., theta oscillation (Mognon et al., 2010).

After artifact rejection, epochs of 4096 ms duration were extracted from the continuous EEG recording. We aimed to keep the trade-off between the number of epochs and the length of epochs optimal. The interval of 4096 ms, which, based on previous studies, we assumed to be sufficient to measure low oscillatory activity (Hillebrand, et al., 2012; Fraschini, et al., 2016). This minimum number was defined as 1/3 of all data in the respective period in order to preserve optimal

signal-to-noise ratio. The average number of trials were similar across periods (Period 1: $M = 99.1$ $SD = \pm 54.7$; Period 2: $M = 88.5$ $SD = \pm 49.7$; Period 3: $M = 98.4$ $SD = \pm 58.9$). Please note that the EEG was segmented regardless of the onsets of the high- and low-probability triplets. Each stimulus was presented for 500 ms, followed by a 120 ms inter-stimulus-interval, while EEG data was segmented into 4096 ms long epochs; therefore, the probability that any EEG epoch consists of different number of responses to high- and low- probability triplets are considered pseudo-randomized.

The EEG was band pass filtered in the delta (0.5-4 Hz), theta (4-7 Hz), alpha low (8-10 Hz), alpha high (10-13 Hz), beta (13-30 Hz), and gamma (30-45 Hz) frequency bands using Hamming windowed finite-impulse-response filter (roll of speed -53dB; maximum bandpass deviation 0.0022). The relative (%) frequency spectra of each band were computed for each participant for all EEG channels and epochs of the given period by the Brainwave software (Version 0.9.58), using Fast Fourier Transform with a window length of 4096 data points (FFT, 10% cosine window) resulting in a 0.25 Hz bin resolution. Relative power was calculated for each frequency band. Relative power of a certain frequency band is defined as a percent of the absolute power (measured in $\mu V^2/Hz$) of the frequency band of interest relative to the absolute power (measured in $\mu V^2/Hz$) summed over the rest of the other frequency bands. Relative spectral power values from each electrode were averaged over ROIs and periods separately for each frequency band.

The strength of FC was calculated between all pairs of EEG channels by measuring phase synchronization using Brainwave software (Version 0.9.58). The strength of FC between any two channels i and j is defined as the phase lag synchronization (phase lag index: PLI). PLI measures the asymmetry of the phase difference distribution (phase of the signal is measured by Hilbert transform function) between two EEG signals, and reflects the consistency by which one signal is

phase leading or phase lagging with respect to another signal (a detailed mathematical description can be found in Stam et al., 2007). PLI has been shown to be sensitive in detecting dynamical changes of phase relationships between different brain regions, and it is insensitive to the effect of volume conduction (effect of common sources of the EEG signal), and also to be (largely) independent of the reference electrode. Random phase differences indicating low connectivity strength are expressed as PLI values around 0, whereas high connectivity strength results in PLI values close to 1. As a result, 128*128 adjacency matrixes (representing all pairwise PLI values between channels) were calculated for each epoch and averaged across subject separately for each learning period of the ASRT task and each frequency band. In order to evaluate FC between brain regions, we performed a region of interest (ROI-based) phase synchronization analysis by computing the average strength of PLI within and between all ROIs. For this analysis, the EEG channels were grouped into 13 ROIs (see in Figure 2): fronto central, lateral frontal, central, lateral central, temporal, parieto central, parietal and occipital (left and right, respectively). All pairwise connectivity strength (PLI) values between channels that belonged to the corresponding pair of ROIs were averaged, which yielded a connectivity value between each ROI pairs separately for each subject and for each period of the task in each frequency band. Similarly, the within-ROI connectivity strength was evaluated by averaging the PLI of the channels pairs that belonged to the same single ROI. As a results, 13 within-ROI connectivity values (e.g., frontal left, temporal right) and 78 values for between-ROI pairs (e.g., between the frontal left and temporal right ROIs) separately for each period of the task and each frequency band were entered in the statistical analysis.

To study the relationship between individual FC across ROIs and overall learning score indices, permutation-based correlation analysis was conducted using a Matlab function (developed by Groppe, Urbach, & Kutas, 2011). Permutation statistics involve examining random

permutations of the data to estimate the null distribution (the distribution of r values that would be expected by chance if the null hypothesis [no relationship between the FC values and behavioral index] was true). The null distribution of the possible Pearson's linear correlation coefficients (r) for these data was obtained by calculating the correlation statistics under rearrangements of the labels on the observed data points.

This function can perform the permutation test simultaneously on multiple variables. When applying the test to multiple variables, the “max statistic” method is used for adjusting the p -values of each variable for multiple comparisons (Blair & Karniski, 1993). This method adjusts p -values in a way that controls the family-wise error rate (across the PLI values for the 78 between-ROI pairs and for the 13 within ROI PLI, separately for each period and each frequency band; similarly to Bonferroni correction). Therefore, this permutation approach provides a solution for the problem of multiple comparisons with improved statistical power (i.e., to achieve a true Type I error rate of .05 with a lower Type II error rate). The analysis was performed separately for each family, between the FC in first, second, and third periods of the ASRT task and the overall learning indices (accuracy and RT).

Permutation test for Pearson's correlation involves the following two steps: First, using the original data (x_i, y_i - which in this case refers to a pairwise FC variable and the corresponding statistical learning index), a new set was defined by randomly (with equal probabilities) assigning values across subjects ($x_i, y_{i'}$, where the i' is a permutation of the set $\{1, \dots, n\}$). In the second step, for each family separately, correlation coefficient r from the randomized data was constructed and the distribution of the correlation coefficients was estimated by permuting the PLI values 5,000 times. From each permutation, the highest (absolute) correlation coefficient was extracted and the p -value was established as the proportion of these correlation coefficients that were higher than or

equal to the observed coefficient. Finally, two-tailed test statistics between permuted and original data was conducted on the corresponding r values.

In order to compare the connectivity-behavior relationship across frequency bands and learning periods, repeated measures analyses of variance were conducted (ANOVAs – see detailed description in the subsection titled “The effect of learning period and frequency band on the relationship between statistical learning performance and FC” of the Results section) separately for FC data of frontal and central ROI and accuracy and RT. Results are corrected and reported as in the case of behavioral results. Post-hoc tests were performed by Bonferroni’s method of pairwise comparisons.

In order to describe the topology of the connectivity-behavior relationship across frequency bands and learning periods, the significant FCs were classified into three larger topological connectivity categories: FCs within fronto-central (anterior) ROIs; FCs between the fronto-central and temporo-parietal ROIs; FCs within temporo-parietal ROIs. Percent of significant FCs relative to all possible connections of the topological connectivity category was calculated separately for each period and frequency band.

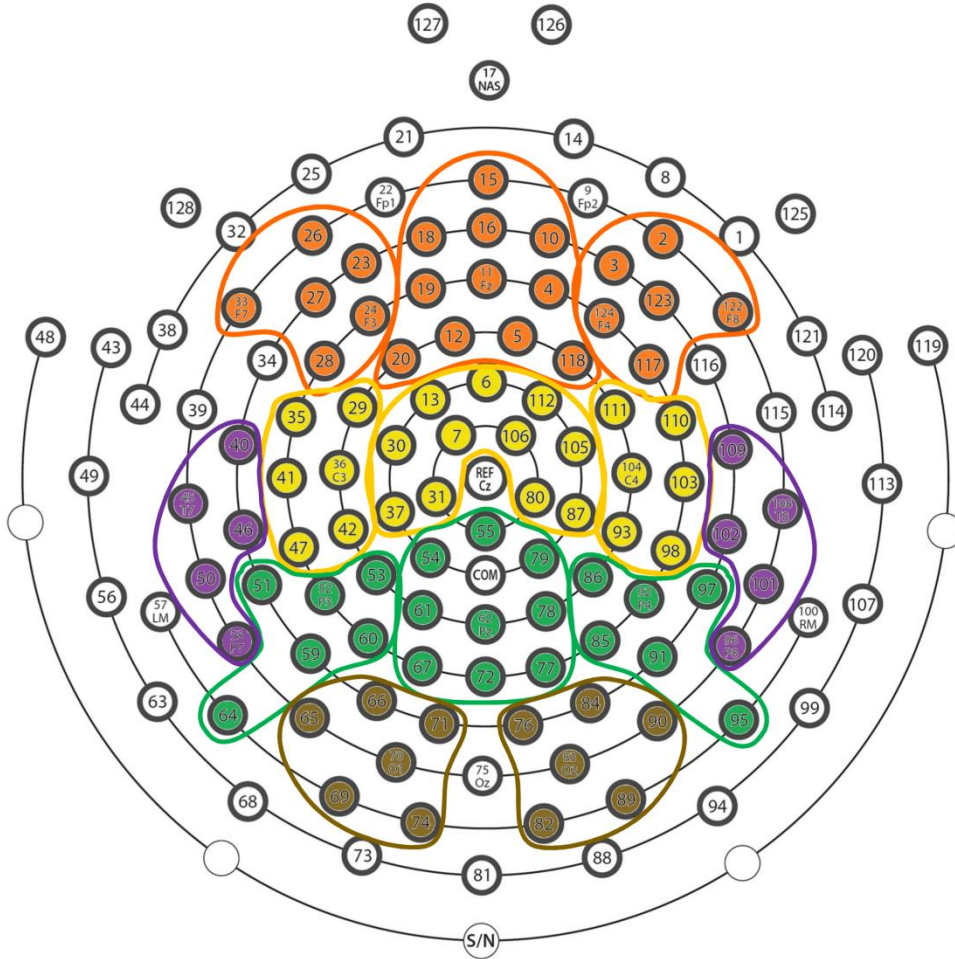


Figure 2. The 128 electrode positions on the scalp. The colors indicate ROIs for left, right, and central regions: orange – frontal, yellow – central, purple – temporal, green – parietal, brown – occipital.

Results

Behavioral results

We performed two-way repeated measures ANOVA for *accuracy* data shown in Figure 3A with TRIPLET (high- vs. low-probability) and PERIOD (1–3) as within-subjects factors. Overall accuracy of participants increased with practice, irrespective of the triplet type (significant main effect of PERIOD, $F(2, 54) = 14.56$, $\varepsilon = .802$, $p < .001$, $\eta_p^2 = .350$), which indicates general skill improvements (significantly higher accuracy in the second and third periods than in the first one,

$ps < .010$). More importantly, participants were more accurate on high- than on low-probability triplets (significant main effect of TRIPLET, $F(1, 27) = 47.23, p < .001, \eta_p^2 = .636$), suggesting statistical learning. In addition, participants became more accurate on high- than on low-probability triplets during the task (significant TRIPLET \times PERIOD interaction, $F(2, 54) = 7.07, p = .002, \eta_p^2 = .207$), showing that statistical learning improved with practice. Namely, the difference between high- and low-probability triplets was significantly larger in the third period than in the first period, $p < .010$, and tended to be larger than in the second one, $p = .086$. Similarly, the difference between high- and low-probability triplets was only a tendency in the first period, $p = .076$, but it was significant in the second and third periods, $ps < .001$, with greater accuracy on high- than on low-probability triplets.

The same ANOVA was performed for *RT* data shown in Figure 3B, yielding results similar to those in the accuracy analysis. Overall *RT* of participants decreased with practice, irrespective of the triplet type (significant main effect of PERIOD, $F(2, 54) = 30.64, \varepsilon = .802, p < .001, \eta_p^2 = .532$), suggesting general skill improvements (significantly faster *RT* in the second and third periods than in the first one, $ps < .001$). More importantly, the main effect of TRIPLET was also significant, $F(1, 27) = 64.50, p < .001, \eta_p^2 = .705$, revealing that participants were faster on high- than on low-probability triplets, which indicates statistical learning. In addition, participants were increasingly faster on high- than on low-probability triplets as the task progressed (significant TRIPLET \times PERIOD interaction, $F(2, 54) = 12.69, p < .001, \eta_p^2 = .320$). The difference between high- and low-probability triplets was significantly larger in the third period than in the first and second periods, $ps < .050$, and this difference tended to be larger in the second period than in the first one, $p = .073$. In the case of the *RT*, the difference between high- and low-probability triplets was significant in all periods, $ps < .010$, with faster responses on high- than on low-probability triplets.

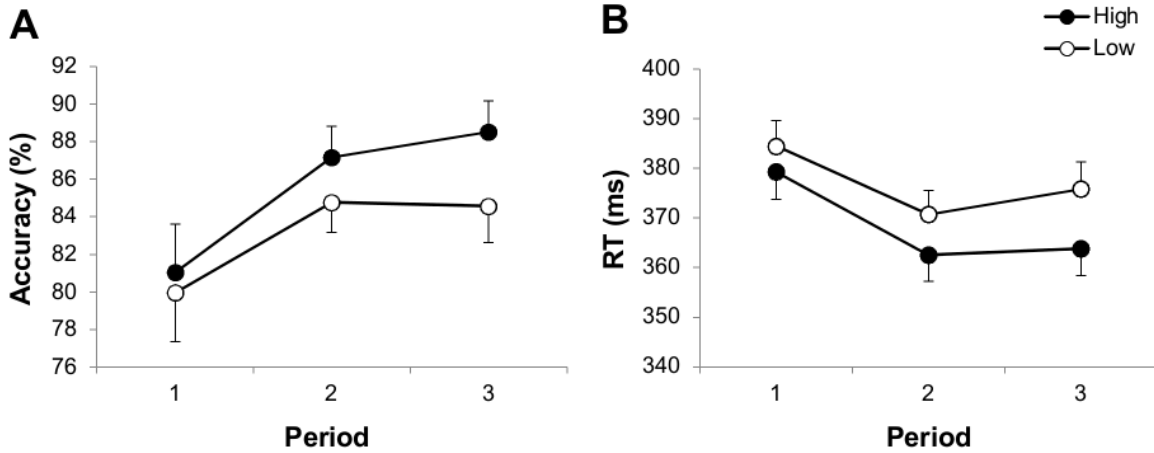


Figure 3. Accuracy (A) and RT for correct responses (B) as a function of period (1-3) and trial type (high- vs. low-frequency triplets). The gap between the curves indicates the statistical learning performance. Error bars denote standard error of mean.

EEG results

Significant correlations were observed only between the individual's connectivity strength in beta and theta frequency bands and the individual's statistical learning scores (accuracy increase and RT decrease for high- relative to low-probability triplets). Results from the connectivity-learning relationship analysis are detailed below and summarized according to the frequency bands in Table 1 and shown in Figure 5-7 (for the correlation coefficients and p values, see Tables S1-S2).

Descriptive characteristics of FC and spectral power

Theta and beta band group average functional connectivity and relative spectral power characteristics are depicted in Figure 4 separately for each ROIs and task periods. Theta band spectral power shows clear fronto-central scalp distribution (lower panel in Figure 4), while beta band power was observed to be stronger at lateral fronto-temporal sites. No change as a function

of period was observed. In line with the spectral density scalp distribution, stronger theta band connectivity was apparent in the fronto-central areas relative to the posterior (temporal and parietal) cortices while in the beta band stronger connectivity was observed in the posterior cortices relative to other areas. The strength of functional connectivity of frontal cortex in theta band tended to be weaker at the third relative to the first period. No apparent change over time was found in the beta band.

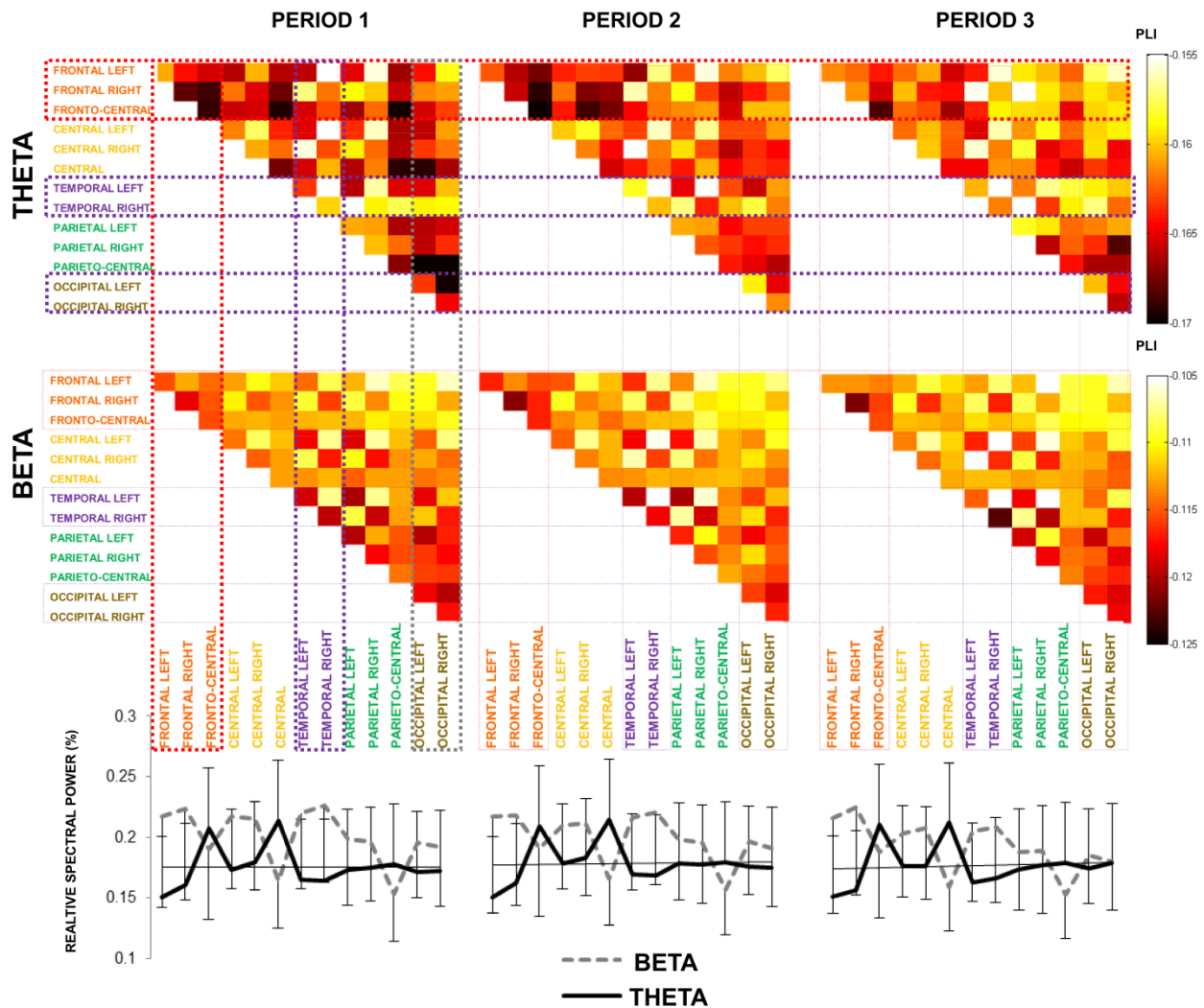


Figure 4. Group average functional connectivity (upper panel) and relative spectral power (lower panel) in theta oscillation (4-7 Hz) and beta oscillation (13-30 Hz) during the ASRT task. Functional connectivity of each ROIs pairs shown as a matrix element separately for task periods (brain lobes highlighted with colors: frontal – red;

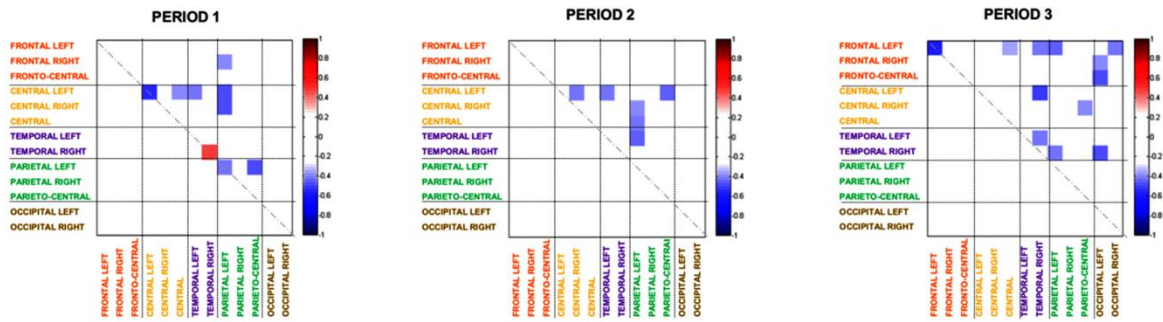
central – yellow; temporal-puple ; parietal- green; occipiral- grey). Color bar indicates PLI value; Spectral power of each ROIs shown on diagrams separately for learning periods. Error bars correspond to standard error of mean.

Relationship between FC and statistical learning

It was hypothesized that the weaker FCs of the fronto-central brain regions would promote the better acquisition of probabilistic information. In line with our hypothesis, significant negative correlation was observed between the statistical learning score (better accuracy for high- than for low-probability triplets) and the theta and beta band FC strength during learning (see Table 1). Thus, in both frequency bands, weaker connectivity was related to better overall learning performance.

Figure 5A shows the contribution of theta oscillation (4-7 Hz) FC to the prediction of overall learning performance measured by accuracy. Significant networks were observed for all periods of the task. Dynamic changes in the brain FC-learning score relationship are further investigated via analysis of the correlation coefficients variances as a function of time (see detailed results below). The set of these connections (N = 6-12 depending on the period) – so called brain networks – associated with statistical leaning consisted of FC with a distinct brain regional distribution. Figure 7 shows the descriptive statistics of learning-related network topology. Considering all three periods, the network predominantly included connections within the fronto-central (anterior) ROIs and connections between the fronto-central (anterior) and temporo-parietal (posterior) ROIs. In addition, an increasing involvement of anterior-posterior connections was evident by the end of the task (Period 3 vs. Period 1). In summary, in line with our hypothesis, the negative relationship between the connectivity and learning performance was due to the contribution of the anterior-posterior functional connections.

A) Correlation between statistical learning measured by accuracy and large scale FC in theta oscillation



B) Correlation between statistical learning measured by RT and large scale FC in theta oscillation

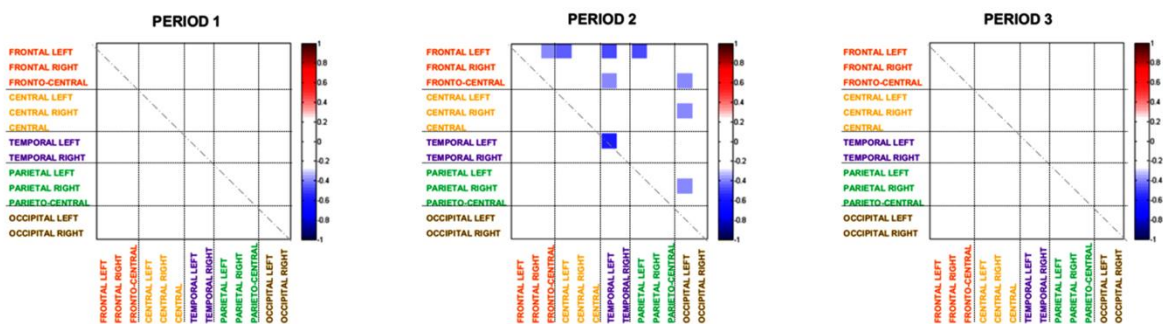
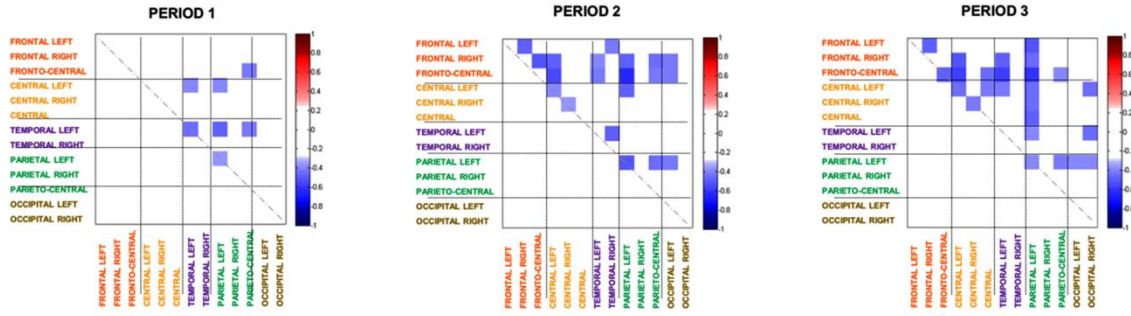


Figure 5. Contribution of theta oscillation (4-7 Hz) functional connectivity to the prediction of overall learning performance measured by accuracy (A) and response time (B). Only significant learning index – functional connectivity correlations are shown separately for periods 1-3 in the matrices between and within the 13 ROIs, respectively. Color bar indicates Pearson's correlation coefficient of the permutation test (r is scaled between 1 and -1; therefore, red color indicates positive and blue color indicates negative relationship between learning and connectivity).

Figure 5B shows the contribution of theta oscillation FC to the prediction of overall learning performance measured by RT. The statistical learning score (faster RTs for high- than for low-probability triplets) was found to be negatively correlated with the FC strength but only in the second period of the task. The topology of this theta band network was characterized by almost equal connections from all brain regions (see Figure 7).

A) Correlation between statistical learning measured by accuracy and large scale FC in beta oscillation



B) Correlation between statistical learning measured by RT and large scale FC in beta oscillation

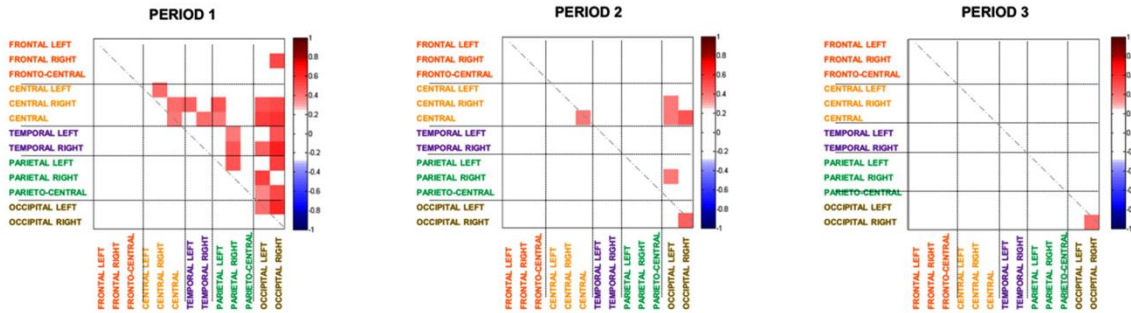


Figure 6. Contribution of beta oscillation (13-30 Hz) functional connectivity to the prediction of overall learning performance measured by accuracy (A) and response time (B). Only significant learning index – functional connectivity correlations are shown separately for periods 1-3 in the matrices between and within the 13 ROIs, respectively. Color bar indicates Pearson's correlation coefficient of the permutation test (r is scaled between 1 and -1; therefore, red color indicates positive and blue color indicates negative relationship between learning and connectivity).

Figure 6A shows the correlation results between the beta oscillation (13-30 Hz) FC and statistical learning score measured by accuracy. Again, the negative relationship between beta band functional connectivity and behavior was evident from the beginning till the last period of the task. These beta band FC-behavior connections were more extended in size ($N = 7-25$) than those in the theta band; the relative contribution of the fronto-central connections in the beta band was

increasing over time (see Figure 7), similarly to the theta band. Thus, the weaker the FC was at the end of the task the better was the overall statistical learning score measured by accuracy.

Figure 6B represents the correlation results between the FC assessed in the beta band and the statistical learning score measured by RT. Exclusively in the beginning of the task significant positive relationship was observed. According to the post hoc topological descriptive statistics, participants with stronger connectivity within the temporo-parietal ROIs showed better learning scores (i.e., responded faster to the high- vs. low-probability triplets) (see Figure 7).

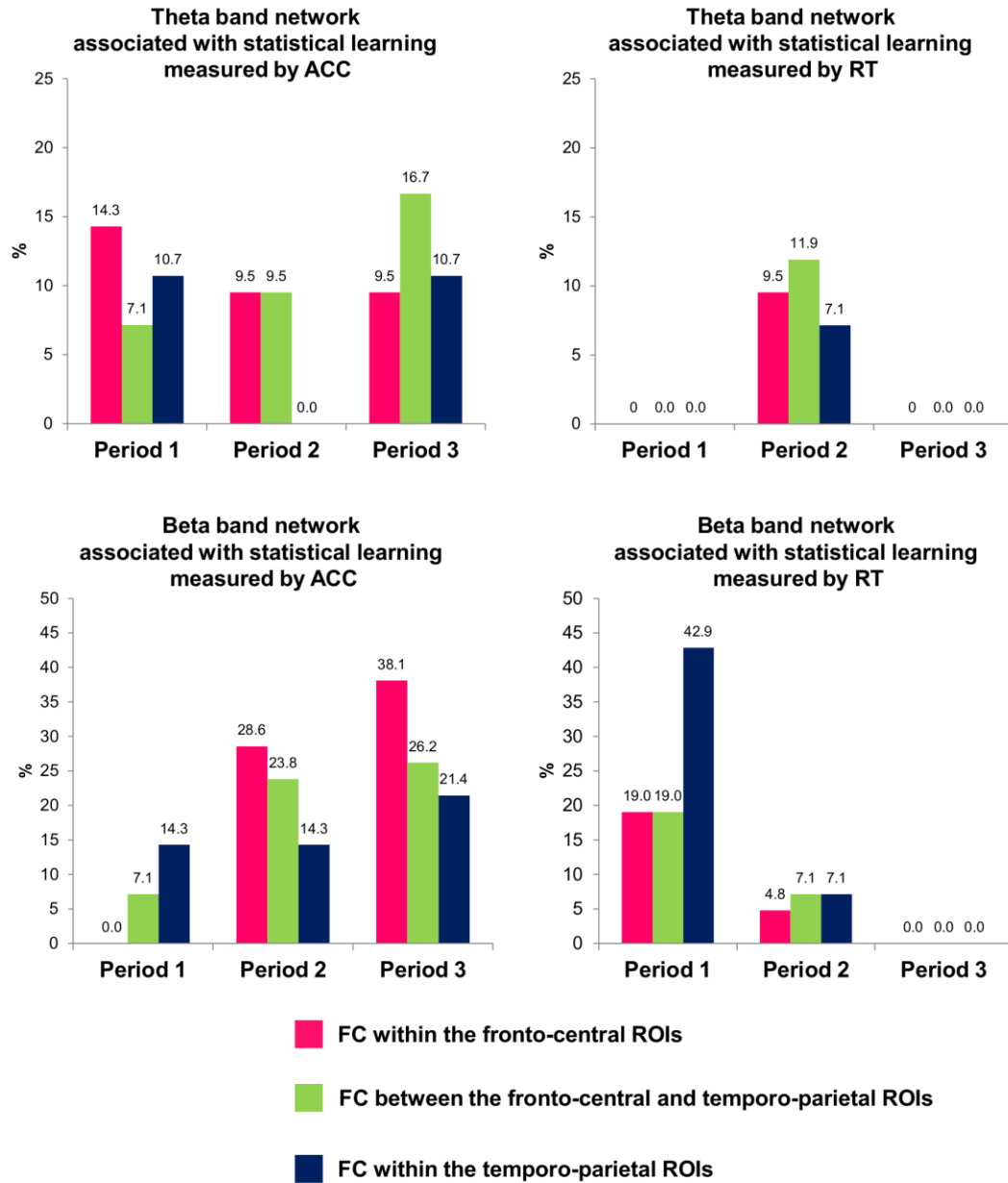


Figure 7. Descriptive statistics of the topographical distribution of beta and theta band functional networks. Significant learning index – functional connectivity correlations are classified according to three types of larger topological connectivity categories: FCs within fronto-central (anterior) ROIs; FCs between the fronto-central and temporo-parietal ROIs; FCs within temporo-parietal ROIs. The descriptive statistics are calculated separately for periods, respectively. Percent of significant FCs relative to all possible connections of the topological connectivity category was calculated separately for each period and frequency band.

It is important to note that the patterns of FC that found to be predictive for behavioral outcome demonstrate 1) frequency specificity, 2) *topography specificity*, 3) statistical learning index specificity, 4) and learning period specificity. With regard to *frequency specificity*, the strength of the FC to the other regions of the brain were significantly correlated with the overall statistical learning indices both in terms of accuracy and RT in theta and beta frequency bands. We did not find reliable amount of significant correlations in the delta, alpha, and gamma frequency bands.

With regard to FC *topography specificity*, in theta oscillation, brain connectivity-behavioral learning performance (accuracy increase as a function of learning) relationship was associated with long-range connectivity between fronto-central and posterior regions (see Figure 5 and Figure 7). Functional connections in beta frequency band associated with perceptual accuracy change due to statistical learning composed of dense interactions of the frontal and central sites (see Figures 6-7). These topographic specific findings are in line with our hypothesis.

With regard to *statistical learning index specificity*, while the accuracy rate of statistical learning was associated with the networks in theta as well as beta oscillations, the RT index of statistical learning was most extensively related to beta connections' strengths in the beginning of the learning session. In addition, the dissociation between networks related to indices of statistical learning was observed in the direction of the significant correlations: Learning, as measured by accuracy, was greater as the strength of FC was lower both in theta and beta frequency bands. In contrast, learning measured by RT was greater as a function of higher connectivity in the beta band, while negative correlations between FC and learning were found in the theta band.

With regard to *learning period specificity*, the strength of theta FC during the first, second, and third periods differentially predicted the learning performance both in terms of accuracy and RT (see Table 1 and following post hoc analysis of learning period effects on correlation

coefficients). For instance, more FCs were related to learning measured by accuracy in the third learning period compared to the previous ones. In contrast, in the case of the RT index, the strength of FC in the second period was more likely associated with learning compared to the other periods. In the beta band, connectivity-learning relationship showed a time period-specific dissociation between accuracy and RT learning measures. In the case of accuracy, more FCs were related to learning in the third period compared to previous ones. In contrast, in the case of RT, more FCs were related to learning in the first period compared to later periods.

Table 1. Results from the connectivity-learning relationship analysis.

		THETA				BETA			
		N	First quartile	Median	Third quartile	N	First quartile	Median	Third quartile
Accuracy	Period 1	10	-.478	-.430	-.362	7	-.466	-.408	-.376
	Period 2	6	-.450	-.417	-.408	20	-.494	-.461	-.424
	Period 3	12	-.498	-.430	-.416	25	-.494	-.445	-.413
RT	Period 1	0	-	-	-	24	.424	.478	.538
	Period 2	9	-.481	-.386	-.383	6	.386	.396	.458
	Period 3	0	-	-	-	1	-	-	-

Note: Results are summarized according to frequency bands. N refers to the number of significant connectivity-learning correlations. For example, in the theta band, 10 PLIs correlate significantly with the accuracy rate of statistical learning in Period 1, and the distribution of correlation values are characterized by the median and the lower and upper quartiles of the r -values.

Temporal dynamics of the relationship between statistical learning performance and FC

In order to investigate the temporal dynamics of the relationship between statistical learning performance and FC, MANOVA was performed for all correlation coefficients (raw r values) – regardless of their significance level – from the correlation analysis between beta and theta connectivity of the frontal and central ROIs and statistical learning indices (measured separately for

ACC and RT), respectively. Specifically, we performed factorial MANOVA on the correlation coefficients (resulted from the accuracy or RT and pairwise FC correlation analysis) with PERIOD (Period 1-3 of the learning task) and ROI (frontal and central) as categorical dependent factors, for theta and beta frequency bands (shown in Figure 8 and Table 2) (for similar analysis, see Fujioka, Mourad, He, & Trainor, 2010). Bonferroni's method was used for correcting the potential Type 1 error in all post hoc comparisons.

The MANOVA performed for connectivity correlation data revealed significant main effect of PERIOD ($F(8, 360) = 23.69, p < .001$; Wilks' Lambda = .43, see also Figure 8). According to the post hoc comparisons: 1) stronger negative correlation between the accuracy rate of learning and FC in the theta band was observed in the third period relative to the first and second periods ($ps < .001$); 2) stronger negative correlation between the RT rate of learning and FC in the theta band was observed in the second period relative to the first and third periods ($ps < .001$); 3) stronger negative correlation between the accuracy rate of learning and beta band FC was observed in the second and in the third periods relative to the first period ($ps < .001$). and 4) stronger positive correlation between the RT learning and beta band FC was observed in the first period relative to the second and third periods ($ps < .001$).

The main effect of ROI was also significant ($F(4, 18) = 9.67, p < .001$ Wilks' Lambda = .82). According to the post hoc comparisons, significant difference was evident between the frontal and central ROIs for the RT learning-theta band FC correlation values: stronger negative correlation was found for the frontal relative to the central ROI ($p = 0.018$). Similarly, accuracy learning-beta band FC correlation values were more negative correlation for frontal relative to central ROI ($p = 0.008$; see Figure 8). In the case of RT learning-beta band FC correlation values, stronger positive correlation was found for central relative to frontal ROI ($p < 0.001$).

Finally, the ROI \times PERIOD interaction was also significant ($F(8, 360) = 3.33, p = .001$; Wilks' Lambda = .87). With respect to accuracy learning-theta band FC, correlation was stronger in the third period relative to the first and the second periods ($ps < .001$) but only in the frontal ROI ($ps < .05$). Similarly, the RT learning-theta band FC correlation was stronger in the second period relative to the first and the third periods ($ps < .001$), again, in the frontal ROI only. Regarding the accuracy learning-beta band FC, stronger correlation was observed for the third relative to the first period both in the frontal and central ROIs ($ps < .001$). In the case of RT learning-beta band FC relationship, stronger positive correlation was found in the first compared to the last period in the frontal and central ROIs ($ps < .001$)

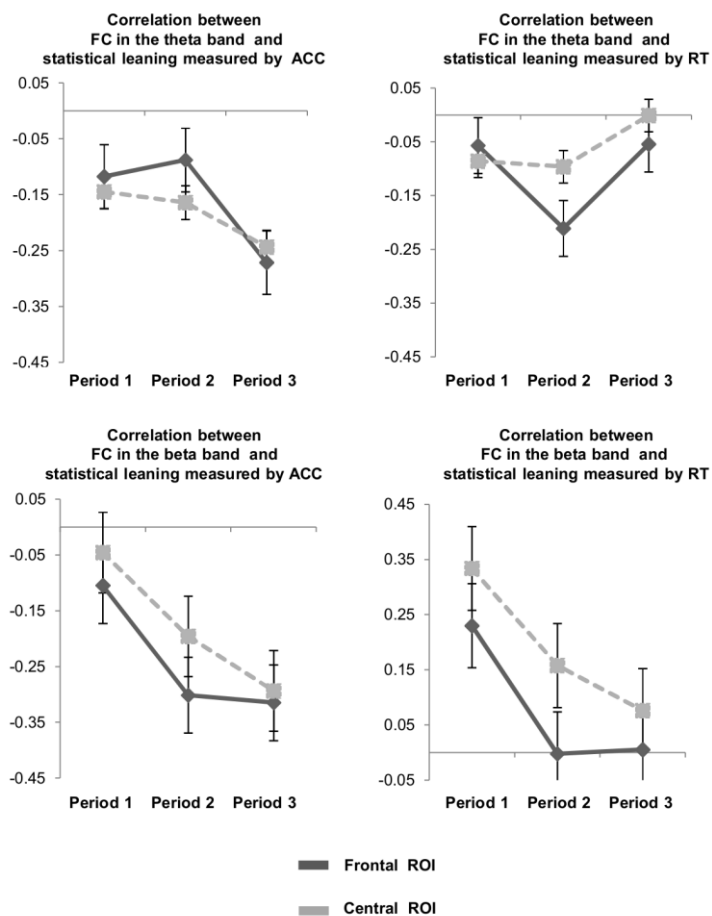


Figure 8. Learning related improvement in accuracy – frontal and central cortical connectivity correlation strength (left panel) and learning related improvement in RT – connectivity correlation strength (right panel)

as a function of period (1-3) and frequency band (theta at the top and beta oscillations at the bottom row). Error bars denote standard error of mean.

Relationship between spectral power and statistical learning

To test whether the observed relationship between statistical learning and the strength of interregional connectivity (phase synchrony) is independent from or related to the task dependent spectral power properties of the brain regions, we calculated correlations between the amplitude (spectral power) of ROIs in beta and theta oscillations and the statistical learning indices. To test the relationship between individual relative power across ROIs and overall learning score indices, permutation-based correlation analysis was performed separately for each period and frequency band power value and each learning index. We observed no significant correlation between the relative amplitude of the theta and beta oscillations in any periods and the learning measures (all $ps > .05$).

Discussion

Here we used EEG FC analysis to test the recruitment of large-scale functional neural circuitry in relation to statistical learning. We investigated the FC patterns that promote learning from initial stages through mastery of sensorimotor regularities. In summary, greater statistical learning score of the accuracy measure was related to the lower strength of connectivity in the theta and beta frequency bands. This negative correlation was found to be greater in the final period of the learning session compared to the first and second periods.

In line with the hypothesis regarding the antagonist role of frontal cortical functions in the progression of statistical learning, our results show that lower connectivity of the anterior sites (in theta and beta oscillations) is related to individual's statistical learning capacity in terms of accuracy: e.g., lower connectivity between the sensorimotor (the central and parietal brain regions) and higher-order cognitive control regions (the frontal cortex) are associated with more efficient statistical learning. In contrast, the FC of beta oscillations predicts learning improvement measured by reaction times: e.g., the connectivity between the sensorimotor network (in the central and parietal brain regions) and visual cortex are associated with superior learning. Additionally, our results highlight that the connectivity-learning relationship varies across early and later stages of acquiring new statistical associations. The positive relationship between beta oscillatory network and behavior is more pronounced at the early stages of learning while the inverse relation between theta band connectivity and behavior is more pronounced at the later stages of the task. Together, our results provide evidence of the dynamic nature of the coupling between cortical regions during learning of statistical regularities, and support the hypothesis that the lower connectivity of the fronto-central control network together with the higher FCs within task-related brain regions are both crucial for the acquisition of novel environmental regularities.

Detection and learning of the statistical regularities in the ASRT task is based on automatic, stimulus-driven processes (Janacsek et al., 2012; Daw et al., 2005): Focusing on external stimuli instead of internally driven, controlled processes leads to better learning. Therefore, the activation and retrieval of previously established internal models from the long-term memory and the use of controlled processes could hinder statistical learning (Nemeth et al., 2013; Virag et al., 2015). Concordantly with the assumed role of theta activity in the top-down attentional processes, the fronto-middle theta oscillations found to be related to the behavioral outcome of learning. Fronto-middle theta oscillations have been linked to prefrontal cortex-dependent cognitive tasks requiring

sustained, internally-directed cognition without external stimuli or responses (Gevins et al., 1997; Hsieh et al., 2011; Jensen & Tesche, 2002; Raghavachari et al., 2001; Scheeringa et al., 2009, Tóth et al., 2014, for reviews see Mitchell et al., 2008). Converging with the present observed fronto-midline spectral power and functional connectivity distribution of the theta rhythm, previous studies identified possible generators of the theta rhythm in the anterior cingulate and medial prefrontal cortices (Gevins et al., 1997; Asada et al., 1999; Onton et al., 2005, Hsieh and Ranganath, 2014).

Recent evidence furthermore suggests that attentional control functions could be realized by theta-band phase synchronization between the fronto-parietal cortices through providing excitatory and inhibitory signals from the frontal to the lower-level areas (for review see Ulhaas & Singer 2006; Clayton et al., 2015). This result can be interpreted as an adaptive neural reorganization where 1) long-term memory processes are downregulated in order to avoid interference coming from previously established internal models, and 2) top-down control functions are reduced in order to focus more on external stimuli, allowing optimal detection and learning of the statistical regularities in the environment.

The inverse relationship between theta FC of the frontal and central cortical ROIs and statistical learning measured by accuracy gradually became stronger from the beginning to the end of the task. In other words, lower theta FC was associated with better statistical learning already in the first period of learning; and it became more extensive for the third period of learning. In contrast, for the learning index assessed by RT, this inverse relationship was observed only in sparse spatial locations and only at the second period of learning, which indicates that theta band FC more reliably follows the behavioral progress in terms of accuracy changes.

Similarly to the observation in the theta rhythm, individual differences in the recruitment of the beta band centro-parietal connectivity were negatively correlated with the accuracy rate of

learning: The more the individuals were able to disband this network (presumably the network consists of the primary and secondary motor and somatosensory brain areas) during the task, the greater the statistical learning was (i.e., fewer errors for high probability triplets compared to the low probability ones). In the case of RT index of learning, beta FC during the beginning of the task was positively correlated with the statistical learning performance (i.e., faster responses for high probability triplets compared to the low probability ones), in the later periods, however, this positive correlation declined or even disappeared. Thus, the temporal trajectory of accuracy-FC and RT-FC relationships show a similar pattern since in the case of both statistical learning measures, correlation with PLIs decreased from Period 1 to Period 3. Oscillatory activity in beta frequency range has been linked to sensory-motor functions (for review see Engel & Fries 2010; Pollok et al., 2014), since in the primary motor cortices pronounced decrease of beta amplitude could be observed during movements, whereas a strong beta power rebound could be seen when movements are executed (for review, see Sauseng & Klimesch 2008). In the present study, the beta power and PLI distribution was observed to be the highest over the lateral positions of frontal and temporal scalp location. Consistently, the dominant source of beta rhythm was localized in primate intracranial EEG recording to the motor and parietal somatosensory cortices (Sanes & Donoghue, 1997). Therefore, the present beta band activity also seems to have motor and sensory cortical origins. Consistent with our results, Serrien, Fisher and Brown (2003) reported a decrease in EEG coherence with practice over the primary sensorimotor cortex during motor skill learning. Alterations of motor-cortical oscillations by means of event-related desynchronization during training on a serial reaction time task has also been recently investigated: The amount of beta-band suppression of spectral power was significantly correlated with the learning performance (Pollok et al, 2014). Our findings are in line with these studies and suggest that lower beta connectivity

and/or decrease in beta connectivity represent a neurophysiological marker of functional cortical reorganization associated with learning.

In contrast to the accuracy measure of statistical learning, RT changes due to learning were observed to be positively correlated with the beta band functional connectivity within the temporo-parietal ROIs. At the beginning of learning, stronger connectivity of the sensory cortices in the beta band was associated with higher gain in statistical learning. This positive relationship may be attributed to the sensorimotor demand of the task. Fast and accurate sensorimotor processing was required already at the very beginning of the task. Concordantly, functional connections of the posterior sites (presumably visual cortices) exclusively associated with learning measured by RT, indicates faster bottom-up evaluation of visual cortical inputs in the case of statistically predictable items. This relationship decreases over time as participants gain more practice. Indeed, the present data suggest that statistical learning may affect accuracy and reaction time (RT) via different cognitive and neural processes: distinct mental operations may contribute to accuracy increase or RT decrease for high- relative to low-probability triplets. Specifically, we speculate that top-down operations reflected in the changes of accuracy with respect to statistical learning while bottom-up sensory-motor operations may contribute to learning-dependent changes of response durations. So far, only behavioral data implicated that statistical learning reflected in RT- and accuracy-based learning indices may operate via different processes (Song 2007a, Song 2007b). Therefore, future studies need to systematically investigate the potential differences in cognitive mechanisms underlying learning indices of accuracy and response durations.

In conclusion, the temporal dynamics of the relationship between statistical learning and FC (i.e., more significant negative correlations as the learning progresses) are in line with neural-efficiency hypothesis (Bassett, Yang, Wymbs, & Grafton, 2015). This idea suggests that “*as learning progresses, the cognitive resources utilized early in learning are no longer needed.*”

Instead, the cortical system will tend to economize resources and limit unnecessary communication and transmission to enable automaticity” (Bassett et al., 2015, pp. 748). Consequently, in the case of statistical learning processes, it could be plausible that the early period of learning is more demanding and it becomes less so as skills reach automaticity by the acquisition of sensorimotor regularities. This idea is supported by prior electrophysiological and brain imaging results showing that 1) language acquisition, which is based on statistical learning, has been negatively correlated with FC between frontal cortices and language related network regions (Chee et al., 2001; Stein et al., 2009; Tatsuno & Sakai, 2005), and 2) the release of a frontal-cingulate in the fronto-parietal network induced by six weeks of training predicts individual differences in learning of sensory-motor skills (Bassett et al. 2011, 2015).

Limitations and future directions

Our findings show relationship between FC and statistical learning. Nevertheless, it is not clear whether this relationship is primarily driven by task-induced changes in FC (state-related characteristics) or by preexisting individual differences (trait-related characteristics). Future studies need to disentangle these two options and their relative contribution to the relationship between FC and learning performance; for example, comparing the association between FC measures in resting state condition versus FC measures during a task with learning performance.

It is important to note that the interpretation of estimated connectivity topology from sensor-level recordings is not straightforward, as the potential localization of the underlying cortical generators are subject to volume conduction effects (Bastos and Schoffelen, 2016; Song et al., 2015). However, PLI measurement used in the present study is not just highly sensitive to true synchrony among brain regions but also has been proven to be a reliable method to minimize the effect of volume conduction (Stam et al., 2007). Also, the topography of FCs shows a distinct

pattern with spatially distant regions (e.g., dominant effects were evident over the sensorimotor cortices) in a highly consecutive manner that has also been observed in previous studies (Serrien & Brown, 2003; Roelfsema et al., 1997; Engel & Fries 2010; Pollok et al., 2014). The relation between the observed spatial patterns in the sensor space and those in the source space is needed to be verified in further research.

The length of analyzed EEG segments may limit the amount of variance of theta rhythm captured relative to higher beta frequency band. It has been reported that longer epoch length results generally in lower connectivity values (Fraschini et al., 2016; Van Diessen et al., 2015). On the one hand, the 4 s window covers at least 8 cycles of the lowest frequency and 32 cycles the highest frequency of the theta band oscillations, which, based on previous studies, we assumed to be sufficient to measure low oscillatory activity (Hillebrand, et al., 2012; Fraschini, et al., 2016). On the other hand, using longer than 4 s window length would have resulted in insufficient number of epochs, which could have led to less optimal trade-off between the number of the epochs and the length of epochs consequently leading stable connectivity and behavior correlation assessment.

It is important to consider the potential effects of fatigue that might have influenced subjects' performance and brain activity. In our study, subjects improved in their general and statistical learning performance over time; therefore, it is unlikely that the observed brain-behavior association merely resulted from changes of state in vigilance. Attention-demanding tasks such as explicit/declarative learning tasks are more likely to be affected by fatigue than implicit statistical learning tasks that are relatively less attention-demanding. Previous studies showed intact implicit statistical learning in populations with weaker attention/executive functions (Brown et al., 2010; Virág et al., 2015), and learning was also intact in demanding dual task conditions (e.g., when computing mathematical additions as a secondary task, see Nemeth et al., 2012). It has also been shown that in the ASRT task, participants remain unaware of the stimulus structure even after

extended practice (e.g., ten days; D. V. Howard et al., 2004). The timing of the task in our study (500 ms stimulus presentation) could make the task even more implicit compared to the previous self-paced versions as participants had even less time to (explicitly) elaborate the stimuli and the connection between subsequent stimuli. Altogether, based on the previous ASRT studies and the results of the verbal reports in the current study, we believe that participants did not gain explicit knowledge of the alternating sequence. Consequently, it is less plausible that fatigue affected our results.

Conclusion

In this study, we used brain connectivity measures of EEG data to investigate the functional communication of large-scale brain networks during statistical learning. To our knowledge, this is the first EEG study investigating statistical learning in the relation of dynamical interregional coupling. In summary, our results imply that learning statistical regularities is accompanied not just by the stronger functional interplay among brain regions but also by the disengagement of frontal cortical circuitry. Our results support a functional role of lower fronto-parietal coupling within the network of theta and beta oscillations in statistical learning. These results provide an integrative and dynamic view of the cortical network during statistical learning.

Funding

This research was supported by the Hungarian Science Foundation (OTKA MB08A 84743, OTKA NF 105878), the Research and Technology Innovation Fund, Hungarian Brain Research Program (KTIA NAP 13-2-2015-0002), Janos Bolyai Research Fellowship of the Hungarian Academy of Sciences (to K.J.), post-doctoral fellowship and internship of Erasmus Mundus Student Exchange Network in Auditory Cognitive Neuroscience (to B.T.), Postdoctoral Fellowship of the Hungarian Academy of Sciences (to A. K. and B.T.).

Acknowledgements

The authors thank for the technical assistance of Elza Fabian. The authors are thankful to Angela D. Friederici, Russell A. Poldrack, Zsolt Turi, Lars Meyer, Ulrike Kuhl, Caroline Beese, and Christopher Steele for comments on the manuscript.

References

Armstrong, B. C., Frost, R., & Christiansen, M. H. (2017). The long road of statistical learning research: past, present and future. *Philosophical Transactions of the Royal Society B: Biological Sciences*, 372(1711).

Asada, H., Fukuda, Y., Tsunoda, S., Yamaguchi, M., & Tonoike, M. (1999). Frontal midline theta rhythms reflect alternative activation of prefrontal cortex and anterior cingulate cortex in humans. *Neurosci Letters*, 274: 29-32.

Aslin, R. N. (2017). Statistical learning: a powerful mechanism that operates by mere exposure. *Wiley Interdisciplinary Reviews: Cognitive Science*, 8(1-2).

Bassett DS, Wymbs NF, Porter MA, Mucha PJ, Carlson JM, Grafton ST. 2011. Dynamic reconfiguration of human brain networks during learning. *PNAS* 108:7641- 7646.

Bassett DS, Yang M, Wymbs NF, Grafton ST. 2015. Learning-induced autonomy of sensorimotor systems. *Nat Neurosci*. 18:744-750.

Bastos AM., Schoffelen J. 2016. A Tutorial Review of Functional Connectivity Analysis Methods and Their Interpretational Pitfalls. *Front. Syst. Neurosci*. 9:175.

Blair RC, Karniski W. 1993. An alternative method for significance testing of waveform difference potentials. *Psychophysiol*. 30:518–524.

- Buzsáki G, Draguhn A. 2004. Neuronal oscillations in cortical networks. *Sci*. 304:1926–1929.
- Buzsáki, G. (2005). Theta rhythm of navigation: link between path integration and landmark navigation, episodic and semantic memory. *Hippocampus*, 15: 827-840.
- Caplan, J. B., & Glaholt, M. G. (2007). The roles of EEG oscillations in learning relational information. *Neuroimage*, 38:604-616.
- Chee MW, Hon N, Lee HL, Soon CS. 2001. Relative language proficiency modulates BOLD signal change when bilinguals perform semantic judgments blood oxygen level dependent. *Neuroimage*. 13:1155–1163.
- Clayton MS, Yeung N, Cohen Kadosh R. 2015. The roles of cortical oscillations in sustained attention. *Trends Cogn Sci*. 19:188-195.
- Cleeremans, A., & McClelland, J. L. (1991). Learning the structure of event sequences. *J Exp Psychol Gen*, 120: 235-253.
- Daw ND, Gershman SJ., Seymour B, Dayan P, Dolan RJ. 2011. Model-based influences on humans' choices and striatal prediction errors. *Neuron*. 69:1204–1215.
- Daw ND, Niv Y, Dayan P. 2005. Uncertainty-based competition between prefrontal and dorsolateral striatal systems for behavioral control. *Nat Neurosci*. 8:1704–1711.
- Delorme, A., Sejnowski, T., & Makeig, S. (2007). Enhanced detection of artifacts in EEG data using higher-order statistics and independent component analysis. *Neuroimage*, 34:1443-1449. doi:10.1016/j.neuroimage.2006.11.004
- Engel AK, Fries P. 2010. Beta-band oscillations - signaling the status quo? *Curr Opin in Neurobiol*. 20:156-165.
- Fell, J, Axmacher N. 2011. The role of phase synchronization in memory processes. *Nat Rev. Neurosci*. 12:105–118.
- Filoteo JV, Lauritzen S, Maddox WT. 2010. Removing the frontal lobes. *Psychol Sci*. 21:415–423.

Fiser J, Berkes P, Orbán G, Máté L. 2010. Statistically optimal perception and learning: from behavior to neural representations. *Trends in Cognitive Science*. 14: 119-130.

Fraschini, M., Demuru, M., Crobe, A., Marrosu, F., Stam, C. J., & Hillebrand, A. (2016). The effect of epoch length on estimated EEG functional connectivity and brain network organization. *JNeural Eng*, 13:036015.

Fujioka T, Mourad N, He C, Trainor LJ. 2011. Comparison of artifact correction methods for infant EEG applied to extraction of event-related potential signals. *Clin Neurophysiol*. 122:43-51.

Gevins A, Smith ME, McEvoy L, Yu D. 1997. High- Resolution EEG mapping of cortical activation related to working memory: effects of task difficulty, type of processing, and practice. *Cerebral Cortex*. 7:374-385.

Groppe DM, Urbach TP, Kutas M. 2011. Mass univariate analysis of event-related brain potentials/fields I: A critical tutorial review. *Psychophysiol*. 48:1711–1725.

Hillebrand, A., Barnes, G. R., Bosboom, J. L., Berendse, H. W., & Stam, C. J. (2012). Frequency-dependent functional connectivity within resting-state networks: an atlas-based MEG beamformer solution. *Neuroimage*, 59:3909-3921.

Howard DV, Howard JH Jr, Japikse K, DiYanni C, Thompson A, Somberg R. 2004. Implicit sequence learning: effects of level of structure, adult age, and extended practice. *Psychol Aging*. 19:79–92.

Howard JH Jr, Howard DV. 1997. Age differences in implicit learning of higher-order dependencies in serial patterns. *Psychol Aging*. 12:634–656.

Hsieh LT, Ekstrom AD, Ranganath C. 2011. Neural oscillations associated with item and temporal order maintenance in working memory. *The J of Neurosci*. 31:10803-10810.

Hsieh LT, Ranganath C. 2014. Frontal midline theta oscillations during working memory maintenance and episodic encoding and retrieval. *Neuroimage*. 85:721-729.

Janacsek K, Fiser J, Nemeth D. 2012. The best time to acquire new skills: age-related differences in implicit sequence learning across the human lifespan. *Dev Sci.* 15:496–505.

Janacsek, K., Ambrus, G. G., Paulus, W., Antal, A., & Nemeth, D. (2015). Right hemisphere advantage in statistical learning: evidence from a probabilistic sequence learning task. *Brain stimulation*, 8:277-282.

Jensen O, Tesche CD. 2002. Frontal theta activity in humans increases with memory load in a working memory task. *Eur J of Neurosci.* 15:1395-1399.

Kikuchi, Y., Attaheri, A., Wilson, B., Rhone, A. E., Nourski, K. V., Gander, P. E., ... & Petkov, C. I. (2017). Sequence learning modulates neural responses and oscillatory coupling in human and monkey auditory cortex. *PLoS Biol*, 15:e2000219.

Klimesch, W., Freunberger, R., Sauseng, P., & Gruber, W. (2008). A short review of slow phase synchronization and memory: evidence for control processes in different memory systems? *Brain research*, 1235:31-44.

Meyer L, Grigutsch M, Schmuck N, Gaston P, Friederici AD. 2015. Frontal-posterior theta oscillations reflect memory retrieval during sentence comprehension. *Cortex.* 71:205–218.

Mitchell, D. J., McNaughton, N., Flanagan, D., & Kirk, I. J. (2008). Frontal-midline theta from the perspective of hippocampal “theta”. *Prog Neurobiol*, 86:156-185.

Mognon A, Jovicich J, Bruzzone L, Buiatti M. 2010. ADJUST: An automatic EEG artifact detector based on the joint use of spatial and temporal features. *Psychophysiol.* 48:229–240.

Nemeth D, Janacsek K, Londe Z, Ullman MT, Howard DV, Howard JH. 2010. Sleep has no critical role in implicit motor sequence learning in young and old adults. *Exp Brain Res.* 201:351–358.

Nemeth D, Janacsek K, Polner B, Kovacs ZA. 2013. Boosting human learning by hypnosis. *Cerebral Cortex.* 23:801–805.

- Onton, J., Delorme, A., & Makeig, S. (2005). Frontal midline EEG dynamics during working memory. *Neuroimage*, 27(2), 341-356.
- Poldrack RA, Clark J, Pare-Blagoev EJ, Shohamy D, CresoMoyano J, Myers C. 2001. Interactive memory systems in the human brain. *Nature*. 414:546–550.
- Pollok B, Latz D, Krause V, Butz M, Schnitzler A. 2014. Changes of motor-cortical oscillations associated with motor learning. *Neurosci*. 275:47-53.
- Raghavachari S, Kahana MJ, Rizzuto DS, Caplan JB, Kirschen MP, Bourgeois B. 2001. Gating of human theta oscillations by a working memory task. *The J of Neurosci*. 21:3175-3183.
- Reber, A. S. (1967). Implicit learning of artificial grammars. *J Verbal Learning Verbal Behav*, 6:855-863.
- Remillard G. 2008. Implicit learning of second-, third-, and fourth-order adjacent and nonadjacent sequential dependencies. *Quarterly J of Exp Psych*. 61:400–424.
- Roelfsema PR, Engel AK, Konig P, Singer W. 1997. Visuomotor integration is associated with zero time-lag synchronization among cortical areas. *Nature*. 385:157-161.
- Sanes JN, Donoghue JP. 1993. Oscillations in local field potentials of the primate motor cortex during voluntary movement. *Proc Natl Acad Sci*. 90:4470-4474.
- Sauseng P, Klimesch W. 2008. What does phase information of oscillatory brain activity tell us about cognitive processes? *Neurosci and Biobehav Rev*. 32:1001–1013.
- Sauseng P, Hoppe J, Klimesch W, Gerloff C, Hummel FC. 2007. Dissociation of sustained attention from central executive functions: local activity and interregional connectivity in the theta range. *Eur J Neurosci*. 25:587–593.
- Schapiro, A. C., Gregory, E., Landau, B., McCloskey, M., & Turk-Browne, N. B. (2014). The necessity of the medial temporal lobe for statistical learning. *J Cog Neurosci*, 26: 1736-1747.

Scheeringa R, Petersson K, Oostenveld R, Norris D, Hagoort P, Bastiaansen M. 2009. Trial-by-trial coupling between EEG and bold identifies networks related to alpha and theta EEG power increases during working memory maintenance. *NeuroImage*. 44:1224-1238.

Schwabe, L., & Wolf, O. T. (2013). Stress and multiple memory systems: from ‘thinking’ to ‘doing’. *Trends Cog Sci*, 17: 60-68.

Serrien DJ, Fisher RJ, Brown P. 2003. Transient increases of synchronized neural activity during movement preparation: influence of cognitive constraints. *Exp Brain Res*. 153:27-34.

Song J., Davey C., Poulsen C., Luu P., Turovets S., Anderson E., Li K., Tucker D.. 2015. EEG source localization: Sensor density and head surface coverage, *J Neurosci Methods*, 256: 9-21

Song S, Howard JH., & Howard DV. 2007b. Sleep does not benefit probabilistic motor sequence learning. *The J of Neurosci*. 27:12475–12483.

Song S, Howard JH., Howard DV. 2007a. Implicit probabilistic sequence learning is independent of explicit awareness. *Learn & Mem*. 14:167–176.

Stam CJ, Nolte G, Daffertshofer A. 2007. Phase lag index: assessment of functional connectivity from multi-channel EEG and MEG with diminished bias from common sources. *Human Brain Map*. 28(11):1178–1193.

Stam CJ., van Straaten ECW. 2012. The organization of physiological brain networks. *Clin Neurophysiol*. 123:1067–1087.

Stein M, Federspiel A, Koenig T, Wirth M, Lehmann C, Wiest R, Strik W, Brandeis D, Dierks T. 2009. Reduced frontal activation with increasing 2nd language proficiency. *Neuropsychologia*. 47:2712–2720.

Stillman, C. M., Gordon, E. M., Simon, J. R., Vaidya, C. J., Howard, D. V., & Howard Jr, J. H. (2013). Caudate resting connectivity predicts implicit probabilistic sequence learning. *Brain Connect*, 3: 601-610.

Tatsuno Y, Sakai KL. 2005. Language-Related Activations in the Left Prefrontal Regions Are Differentially Modulated by Age, Proficiency, and Task Demands. *The J of Neurosci.* 25:1637–1644.

Tóth B, Kardos, Zs, File B, Boha R, Stam CJ, Molnár M. 2014. Frontal midline theta connectivity is related to efficiency of WM maintenance and is affected by aging. *Neurobiol of Learn and Mem.* 114:58–69.

Uhlhaas PJ, Singer W. 2006. Neural synchrony in brain disorders: relevance for cognitive dysfunctions and pathophysiology. *Neuron.* 52:155-68.

Van Diessen, E., Numan, T., Van Dellen, E., Van Der Kooi, A. W., Boersma, M., Hofman, D. & Stam, C. J. (2015). Opportunities and methodological challenges in EEG and MEG resting state functional brain network research. *Clin Neurophysiol*, 126:1468-1481.

Varela F, Lachaux J, Rodriguez E, Martinerie J. 2001. The brainweb: Phase synchronization and large-scale integration. *Nat Rev Neurosci.* 2:229-239.

Virag M, Janacsek K, Horvath A, Bujdosó Z, Fábó D, Nemeth D. 2015. Competition between frontal lobe functions and implicit sequence learning: evidence from the long-term effects of alcohol. *Exp Brain Res.* 233:2081-2089.

Supplementary Information to the manuscript entitled Dynamics of EEG functional connectivity during statistical learning

Table S1. Results of the theta band connectivity-behavior relationship analysis.

	Frontal left	Frontal right	Fronto-central	Central left	Central right	Central	Temporal left	Temporal right	Parietal left	Parietal right	Parieto-central	Occipital left	Occipital right
Frontal left	Period 3 r = -.568 p = .001		Period 2 r = -.385 p = .046	Period 2 r = -.456 p = .016			Period 2 r = -.493 p = .008			Period 2 r = -.469 p = .01			
Frontal right													
Fronto-central							Period 2 r = -.385 p = .048					Period 2 r = -.381 p = .039	
Central left				Period 1 r = -.537 p = .002									
Central right				Period 2 r = -.414 p = .028								Period 2 r = -.379 p = .044	
Central	Period 3 r = -.362 p = .049			Period 1 r = -.405 p = .032			Period 2 r = -.585 p = .001						
Temporal left				Period 1 r = -.430 p = .019									
				Period 2 r = -.424 p = .022									
Temporal right	Period 3 r = -.419 p = .027			Period 3 r = -.517 p = .004			Period 3 r = -.429 p = .023	Period 1 r = .490 p = .009					
Parietal left	Period 3 r = -.462 p = .011	Period 1 r = -.375 p = .043		Period 1 r = -.472 p = .008	Period 1 r = -.479 p = .008	Period 2 r = -.416 p = .030	Period 2 r = -.454 p = .012	Period 3 r = -.421 p = .021	Period 1 r = -.434 p = .021				
					Period 2 r = -.390 p = .034								
Parietal right												Period 2 r = -.386 p = .050	
Parieto-central				Period 2 r = -.449 p = .017	Period 3 r = -.404 p = .033				Period 1 r = -.478 p = .01				
Occipital left		Period 3 r = -.387 p = .040	Period 3 r = -.498 p = .007					Period 3 r = -.471 p = .008					
Occipital right	Period 3 r = -.416 p = .023												

Note: The significant correlation results between the RT learning index and PLI of ROIs are presented above the diagonal (blue area), while results of the correlation analysis between the accuracy learning index and PLI of ROIs are presented under the diagonal (yellow). In the diagonal (white area), RT results are presented with blue letters, accuracy results are presented with yellow letters.

Table S2. Results of the beta band connectivity-behavior relationship analysis.

	Frontal left	Frontal right	Fronto-central	Central left	Central right	Central	Temporal left	Temporal right	Parietal left	Parietal right	Parieto-central	Occipital left	Occipital right
Frontal left													
Frontal right	Period 2 r = -.492 p = .009 Period 3 r = -.480 p = .011					Period 1 r = .367 p = .042							Period 1 r = .529 p = .005
Fronto-central		Period 2 r = -.504 p = .006	Period 3 r = -.473 p = .008										
Central left	Period 3 r = -.360 p = .050	Period 2 r = -.490 p = .007 Period 3 r = -.515 p = .002	Period 2 r = -.557 p = .002 Period 3 r = -.589 p = .002	Period 2 r = -.397 p = .032 Period 3 r = -.445 p = .013	Period 1 r = .422 p = .026								Period 2 r = .469 p = .014
Central right					Period 2 r = -.375 p = .049 Period 3 r = -.412 p = .027	Period 1 r = .408 p = .029	Period 1 r = .457 p = .015		Period 1 r = .490 p = .003			Period 1 r = .481 p = .010 Period 2 r = .396 p = .031	Period 1 r = .523 p = .005
Central		Period 3 r = -.375 p = .046	Period 3 r = -.438 p = .017	Period 3 r = -.422 p = .021		Period 1 r = .406 p = .034 Period 2 r = .389 p = .036		Period 1 r = .434 p = .022	Period 1 r = .400 p = .030			Period 1 r = .562 p = .001 Period 2 r = .378 p = .046	Period 1 r = .577 p = .008 Period 2 r = .469 p = .009 Period 1 r = .493 p = .006
Temporal left		Period 2 r = -.376 p = .046 Period 3 r = -.497 p = .006	Period 2 r = -.430 p = .019 Period 3 r = -.587 p < .001	Period 1 r = -.382 p = .034 Period 3 r = -.421 p = .024			Period 1 r = -.466 p = .005				Period 1 r = .376 p = .045		
Temporal right	Period 2 r = -.437 p = .020 Period 3 r = -.527 p = .002						Period 2 r = -.479 p = .009			Period 1 r = .471 p = .012 Period 1 r = .475 p = .008		Period 1 r = .465 p = .017	Period 1 r = .637 p < .001 Period 1 r = .541 p = .003
Parietal left		Period 2 r = -.486 p = .011 Period 3 r = -.464 p = .008	Period 2 r = -.635 p < .001 Period 3 r = -.615 p < .001	Period 1 r = -.376 p = .030 Period 2 r = -.494 p = .009 Period 3 r = -.448 p = .014	Period 3 r = -.440 p = .020	Period 3 r = -.492 p = .009	Period 1 r = -.484 p = .003 Period 3 r = -.391 p = .036		Period 1 r = -.363 p = .031 Period 2 r = -.511 p = .006 Period 3 r = -.377 p = .037				
Parietal right												Period 1 r = .557 p = .003 Period 2 r = .396 p = .031 Period 1 r = .373 p = .046	
Parieto-central		Period 2 r = -.468 p = .008	Period 1 r = -.421 p = .020 Period 2 r = -.436 p = .019 Period 3 r = -.403 p = .029				Period 1 r = -.409 p = .028		Period 2 r = -.454 p = .009 Period 3 r = -.413 p = .025				Period 1 r = .512 p = .005

Occipital left	Period 2 r = -.432 p = .024	Period 2 r = -.422 p = .022	Period 2 r = -.420 p = .021	Period 3 r = -.393 p = .024	Period 3 r = -.386 p = .036	Period 1 r = .430 p = .021	Period 1 r = .614 p < .001
Occipital right		Period 3 r = -.439 p = .012	Period 3 r = -.468 p = .011				Period 1 r = .494 p = .006
							Period 2 r = .454 p = .016
							Period 3 r = .423 p = .023

Note: The significant correlation results between the RT learning index and PLI of ROIs are presented above the diagonal (blue area), while results of the correlation analysis between the accuracy learning index and PLI of ROIs are presented under the diagonal (yellow). In the diagonal (white area), RT results are presented with blue letters, accuracy results are presented with yellow letters.